

Kinetics of the Cl(²P_J) + CH₄ Reaction: Effects of Secondary Chemistry below 300 K

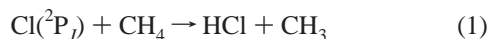
J. J. Wang and Leon F. Keyser*

*Atmospheric Chemistry Element, Earth and Space Sciences Division, Jet Propulsion Laboratory, California Institute of Technology, Pasadena, California 91109**Received: April 22, 1999; In Final Form: July 22, 1999*

Absolute rate data for the Cl(²P_J) + CH₄ → HCl + CH₃ reaction have been obtained from 218 to 298 K by using the discharge flow resonance fluorescence technique in helium at 1 Torr total pressure. The result at 298 K is (10.1 ± 0.6) × 10⁻¹⁴ cm³ molecule⁻¹ s⁻¹. The temperature dependence in Arrhenius form is (6.5 ± 0.9) × 10⁻¹² exp[(-1235 ± 34)/T]. The errors given are one standard deviation; overall experimental error is estimated at ±15%. Because of the relatively large disagreement among earlier measurements at low temperatures, the results were examined for possible effects of non-Boltzmann spin distribution and vibrational excitation of CH₄, secondary chemistry of CH₃ radicals, and impurities in the Cl atom and CH₄ sources. There was no significant change in the observed rate constant when an efficient spin quencher, CF₄, was added, and estimates indicate that vibrational partitioning in CH₄ should be at the ambient reactor temperature before the start of the reaction. The results were also independent of the source of Cl atoms (microwave discharge or thermal decomposition of Cl₂) and whether CH₄ was purified in situ. However, the observed rate constant did depend on initial Cl atom concentrations and to a lesser extent on CH₄ concentrations. Numerical simulations were used to assess the importance of secondary chemistry over a range of reactant concentrations.

Introduction

In the atmosphere from 15 to 50 km the reaction of atomic chlorine with methane is the major pathway by which reactive



chlorine is converted to the relatively inert reservoir species, HCl.¹ During winter in the polar regions, abnormally high levels of reactive chlorine can be formed by reactions initiated on the surfaces of stratospheric clouds. In many cases, reaction 1 also controls the recovery rate from this perturbed condition to a normal partitioning of reactive and reservoir chlorine species.^{2–8} The Cl + CH₄ reaction also has a major influence on the isotopic composition of CH₄ and CO in the stratosphere.^{9–11}

Because of its importance, reaction 1 has been the subject of many studies using various experimental techniques over a wide temperature range.^{12,13} For the present study of Cl + CH₄ applied to stratospheric chemistry, we will consider only temperature-dependent studies below 300 K. In this region there have been several determinations of the absolute rate constant: three studies using the discharge flow resonance fluorescence technique under laminar^{14,15} or turbulent¹⁶ flow conditions; one study using discharge flow mass spectrometry;¹⁷ one study using the very-low-pressure reactor technique;¹⁸ and four studies using flash photolysis resonance fluorescence.^{19–22} In this temperature range, there are also two measurements that used competitive chlorination^{17,23} to obtain the Cl + CH₄ rate constant relative to Cl + C₂H₆; to convert to absolute values we use 7.7 × 10⁻¹¹ exp(-90/T) cm³ molecule⁻¹ s⁻¹ for the C₂H₆ rate constant.¹² Within each technique the agreement is good over the entire temperature range; but the competitive chlorination experiments

yield linear Arrhenius plots above and below room temperature while the other techniques observed nonlinear plots. At 298 K these various methods agree within 6–13%; this is within the experimental uncertainties of ±15 to ±20%. However, at 220 K the averages of the discharge flow (including the very-low-pressure reactor data) and the flash photolysis results are higher than the competitive chlorination results by about 15% and 35%, respectively. This disagreement is at the margin of the combined experimental uncertainties and might not be significant. But the agreement among the studies within each technique combined with the rather large discrepancies at low temperatures suggests that systematic errors may be present in the low-temperature studies of Cl + CH₄ by one or more of these techniques.

Several possibilities exist that could account for the disagreement at low temperatures. Nonequilibrium between the atomic chlorine spin states (²P_{1/2} and ²P_{3/2}) has been suggested.²¹ Since vibrational excitation of CH₄ can greatly increase the rate of reaction,^{24,25} incomplete vibrational relaxation at low temperatures could lead to observed rate constants that are too high. Observed decays of atomic chlorine could also be affected by secondary reactions (eqs 2–3) of molecular and atomic chlorine with the methyl radicals produced by reaction 1.^{15,16} Reaction



of hydrogen atom impurities (eq 4) in the chlorine atom source could interfere by regenerating chlorine atoms.¹⁵ Competition



for chlorine atoms by residual ethane (eq 5) in the methane source could interfere especially at low temperatures.

* To whom correspondence should be addressed. Fax: (818) 393-5019. E-mail: Leon.F.Keyser@jpl.nasa.gov.

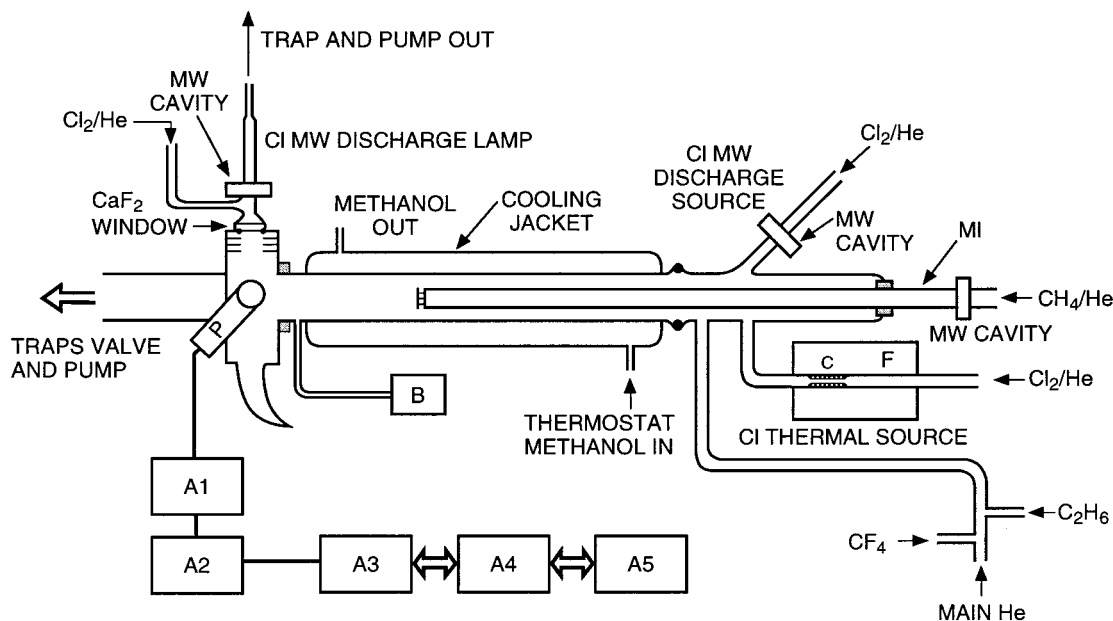
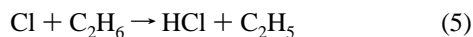


Figure 1. Schematic diagram of discharge flow resonance fluorescence apparatus: B—Baratron pressure gauge (1–10 Torr); MI—movable injector for addition of $\text{CH}_4 + \text{He}$ during $\text{Cl} + \text{CH}_4$ kinetics runs, $\text{F}_2 + \text{He}$ during Cl atom calibration runs, and $\text{Cl}_2 + \text{He}$ during Cl atom wall loss runs; F—furnace; C—capillary tube; P—photomultiplier with BaF_2 filter; A1—fast-preamplifier; A2—amplifier/discriminator; A3—dual counter/timer; A4—interface; A5—computer.



The purpose of the present study is to test the discharge flow resonance fluorescence technique for possible effects of secondary chemistry at temperatures below 300 K where the disagreement among the previous studies is worst. To check for spin equilibration, an efficient spin quencher, CF_4 , is added to the $\text{Cl} + \text{CH}_4$ reaction system. Vibrational deactivation is discussed in terms of known quenching rate constants. To test for possible secondary chemistry involving methyl radicals, initial concentrations of atomic chlorine and methane are varied over wide ranges. Since in the present study atomic chlorine is the limiting reactant ($[\text{Cl}]_0 \ll [\text{CH}_4]$), methyl radical concentrations and, thus, the importance of reactions 2 and 3 can be controlled by varying the initial chlorine atom concentrations. To check for impurities in the chlorine atom source and possible interference from reaction 4, chlorine atoms are generated by using a microwave discharge or thermal dissociation. Ethane impurities in methane are minimized by using research grade methane and by further purifying it in situ to double check for impurities possibly added in the connecting vacuum lines. Finally a numerical model is used to assess the importance of secondary chemistry at varying concentrations of chlorine atoms and methane.

Experimental Section

The present study was carried out by using a fast flow system with resonance fluorescence detection. A schematic diagram of the apparatus is presented in Figure 1. The experimental approach is similar to that used in a previous study,¹⁵ and only important modifications will be discussed in detail.

Reactor. The temperature-controlled Pyrex reactor has an internal diameter of 5.04 cm and is 60 cm in length. At the downstream end, it is connected by means of an epoxy seal to a stainless steel resonance fluorescence cell. Pressure is measured by using a 10 Torr capacitance manometer connected to a port between the reactor and the fluorescence cell. At the upstream end are connections to microwave and thermal sources

of Cl atoms, a fixed inlet for the He carrier, and a movable inlet for $\text{CH}_4 + \text{He}$. The inner surface of the reactor and outer surface of the movable inlet are coated with halocarbon wax (Series 15–00, Halocarbon Corp.) to minimize wall loss of Cl atoms. The main helium carrier flow bypasses the discharge to minimize production of impurity atoms such as H or O . Total helium flow rates are around 1900 to 2100 $\text{cm}^3 \text{min}^{-1}$ at STP to establish flow velocities of 1000 to 1500 cm s^{-1} . The flow system is pumped by a trapped 38 L s^{-1} rotary pump; a throttling valve is used to maintain a total pressure around 1 Torr at the above flow velocities. Methane is added through a 1.5 cm o.d. movable injector at flow rates from 30 to 290 $\text{cm}^3 \text{min}^{-1}$ at STP. Other ports upstream of the reactor allow various reagents, such as CF_4 , C_2H_6 , Cl_2 , H_2 , and F_2 , to be added as needed to the reactor tube. Temperatures in the reaction zone were maintained within ± 2 K by using refrigerated bath circulators (Neslab, ULT-80DD or RTE-110) to pass heat exchange fluids (water or methanol) through the cooling jacket. Temperatures were monitored by two thermocouples (Type E, chromel–constantan) located inside each end of the cooling jacket.

Atomic Chlorine Sources. Chlorine atoms are generated in dilute mixtures of Cl_2 in He by using a microwave (2.45 GHz) discharge or thermal decomposition. An uncoated 1 cm i.d. Suprasil quartz tube is used in the microwave source, which is operated at 60 W. Total flow rates are about 300 $\text{cm}^3 \text{min}^{-1}$ at STP and the pressure is about 1 Torr. Typically 43 to 55% dissociation efficiencies are obtained at Cl atom concentrations 6.8×10^9 to 4.1×10^{11} atoms cm^{-3} .

For the thermal dissociation source, we use a 1 cm i.d. quartz tube with a capillary region, 0.62 mm i.d. by 4 cm in length located near the downstream end of a tubular shaped furnace, which is operated at 1325 K and monitored by a thermocouple (Type K, chromel–alumel). The heated section of the tube is uncoated, but immediately downstream the walls are coated with phosphoric acid. Total flow rates are about 450 $\text{cm}^3 \text{min}^{-1}$ at STP and the total pressure is approximately 400 Torr. Dissociation efficiencies are 25 to 34% for Cl atom concentrations 9.6×10^{10} to 2.8×10^{11} atoms cm^{-3} .

Atomic Chlorine Detection. Cl atoms are detected by resonance fluorescence immediately downstream of the reactor. The fluorescence is excited by radiation from a 50 W microwave discharge in a chlorine resonance lamp. A mixture of about 0.5% Cl₂ in helium is passed through the lamp at pressures near 1.5 Torr. The resonantly emitted photons are detected at a 90° angle to the lamp by means of a photomultiplier, PMT, (EMR 541G-08–18) sensitive between 105 and 220 nm. A barium fluoride filter window is placed before the PMT to cut off radiation below 136 nm and eliminate interference from oxygen and hydrogen atom impurities. In this spectral region a strong chlorine transition occurs near 139 nm. As shown in Figure 1, the output of the PMT is fed to a photon counting system and then to a computer by a standard RS-232 interface. The scattered signal is significantly reduced by using light baffles in front of the chlorine atom lamp and the PMT and Wood's horns at positions opposite to the lamp and the PMT. During the Cl + CH₄ runs, background fluorescence signals were determined with the Cl₂ flow turned off, discharge or furnace on, and C₂H₆ added to scavenge any residual Cl atoms.

Atomic Chlorine Calibration. The Cl atom detection sensitivity is calibrated by generating a known amount of Cl atoms either from the reaction $F + Cl_2 \rightarrow Cl + FCl$ ($k = 1.6 \times 10^{-10} \text{ cm}^3 \text{ molecule}^{-1} \text{ s}^{-1}$ at room temperature²⁶) or from $H + Cl_2 \rightarrow Cl + HCl$ ($k = 2.6 \times 10^{-11} \text{ cm}^3 \text{ molecule}^{-1} \text{ s}^{-1}$ ^{27,28}); in both cases, the F atoms or H atoms are produced in a microwave discharge and used in large excess over known concentrations of Cl₂. The observed signals contain contributions from Cl atom fluorescence produced by the calibrating reactions and fluorescence from other background sources of Cl atoms and from scattered light. The sum of the background and scattered signals is determined by turning off the Cl₂ flow. Semilog plots of the calibration signal vs the reaction length are linear, and loss of Cl atoms is accounted for by extrapolating these plots to the detector position with a linear least-squares analysis. The two methods agree within 5 to 25%. Since lower background losses are observed in the F atom reaction, it is used in most of the calibrations. Typical detection sensitivities are about $8.0 \times 10^{-8} \text{ counts s}^{-1}/\text{atoms cm}^{-3}$ with background signals at about $380 \text{ counts s}^{-1}$. For a typical 50 s counting time, this is equivalent to a minimum detectable [Cl] of $5 \times 10^7 \text{ atoms cm}^{-3}$ at a signal-to-noise ratio of unity. Plots of fluorescence signal vs [Cl] are linear over the entire range studied from about 2×10^9 to $3 \times 10^{11} \text{ atoms cm}^{-3}$.

Chlorine Atom Wall Loss. Since Cl atoms are added and detected at fixed points, wall losses are not directly observed in our experiments, but they are needed for the diffusion corrections and numerical simulations described below. These measurements are performed under the same conditions of temperature, pressure, and flow velocity as those used in the Cl + CH₄ experiments, except, of course, without added CH₄. Cl atoms are formed in a microwave discharge of Cl₂ + He in the movable inlet and added at various reaction lengths. The resulting linear semilog plots of the fluorescence signals vs length show that the wall loss is first order in [Cl]. A linear least-squares analysis is then used to obtain the wall loss rate constants from the slopes of these plots. After diffusion corrections the values observed (\pm one standard deviation) are $11.7 (\pm 2.9)$, $14.0 (\pm 4.1)$, and $4.2 (\pm 2.8) \text{ s}^{-1}$ at 218, 261, and 298 K, respectively.

Calibrations. All mass flow controllers and meters were calibrated for N₂, He, or CH₄ by using the volume change at constant pressure (bubble meter) method or by the pressure rise at constant volume method. Pressure gauges were calibrated

by reference to an oil manometer. All thermocouples used in the experiments were calibrated at 273 and near 195 K by using ice plus water and CO₂ plus methanol baths, respectively. Barometric corrections were used to obtain the CO₂ equilibrium temperature. The temperature in the reaction zone was measured by using a thermocouple probe in place of the movable inlet. At low temperatures the probe reading was 1 to 2 K lower than the two thermocouples in the cooling jacket, while at 298 K the probe temperature was within 0.2 K. All temperatures reported are based on the probe readings.

Corrections. The data were corrected for the viscous pressure drop between the reaction zone and the pressure measurement port.²⁹ Pressure corrections were less than 0.5%. Observed pseudo-first-order rate constants were also corrected for axial and radial diffusion by using the method described previously.^{30,31} For these corrections a value of $0.0237 \times T^{1.75} \text{ Torr cm}^2 \text{ s}^{-1}$ was used for the diffusion coefficient of Cl atoms in He.³² Diffusion corrections ranged from 2 to 14% at all temperatures studied.

Reagents. Gases used were chromatographic grade He (99.9999%), research grade Cl₂ (99.99%), Matheson research grade CH₄ (99.99%), CF₄ (99.9%), H₂ (99.9995%), a 10.33% mixture of C₂H₆ in He and a 1% mixture of F₂ in He. He was further purified by passage through a molecular sieve (Linde 3A) trap at 77 K just prior to use. CH₄ was purified in situ as described below.

Results

The present experiments were carried out with methane in large excess at temperatures between 218 and 298 K. Helium was used as the carrier gas at total pressures of $(1.02 \pm 0.02) \text{ Torr}$. Molecular chlorine, Cl₂, was added at concentrations from 1.1×10^{10} to $4.1 \times 10^{11} \text{ molecules cm}^{-3}$; after dissociation by microwave discharge or thermal decomposition, this resulted in initial chlorine atom concentrations, [Cl]₀, from 6.8×10^9 to $4.1 \times 10^{11} \text{ atoms cm}^{-3}$. Methane concentrations were between 5.7×10^{14} and $4.5 \times 10^{15} \text{ molecules cm}^{-3}$. Initial stoichiometric ratios, [CH₄]/[Cl]₀, ranged from 4.8×10^3 to 1.6×10^5 . Under these conditions, the loss of atomic chlorine is pseudo-first-order and may be written

$$-d[\text{Cl}]/dt = k_1[\text{CH}_4][\text{Cl}] + k_L[\text{Cl}] \quad (6)$$

Since the Cl atom resonance fluorescence intensity, $I(\text{Cl})$, was found to vary linearly with [Cl], we can write

$$k_+ \equiv -d \ln[I(\text{Cl})]/dt = k_1[\text{CH}_4] + k_L \quad (7)$$

where k_+ is the total first-order rate constant for loss of atomic chlorine with CH₄ added through the movable injector, k_1 is the bimolecular rate constant for reaction 1, and k_L accounts for changes in the Cl atom signal other than by reaction with CH₄. The latter effect is due to changes in the flow velocity, Cl atom wall loss, and reaction with impurities in the He carrier gas up and down stream of the movable injector. Values of k_+ were determined from the slopes of $\ln[I(\text{Cl})]$ vs l plots by linear least-squares analysis when CH₄ was present; here l is the reaction length, which under plug flow conditions determines the reaction time, $t = l/v$, where v is the average flow velocity. Reaction lengths were 4 to 26 cm and reaction times ranged from 2.7 to 26 ms. The range of Cl atom decays depended on [CH₄] and the temperature; between these reaction times the decays were from about $e^{-0.4}$ to $e^{-4.0}$. Most semilog plots of the Cl decay were linear over the entire range; if nonlinearity

TABLE 1: Summary of Observed Rate Constants for Cl + CH₄

T (K)	runs	k_1 (10 ⁻¹⁴ cm ³ molecule ⁻¹ s ⁻¹)	
		average ^{a,b}	slope ^{a,c}
298	24	10.1 ± 0.60	10.2 ± 0.20
279	12	7.56 ± 0.70	6.28 ± 0.48
261	38	5.98 ± 0.43	6.46 ± 0.18
239	13	3.69 ± 0.20	3.49 ± 0.10
218	29	2.20 ± 0.28	2.25 ± 0.08

^a Errors are one standard deviation. ^b Average of individual $k_1'/[\text{CH}_4]$.
^c From plots of $k_1' = k_1[\text{CH}_4]$ vs $[\text{CH}_4]$.

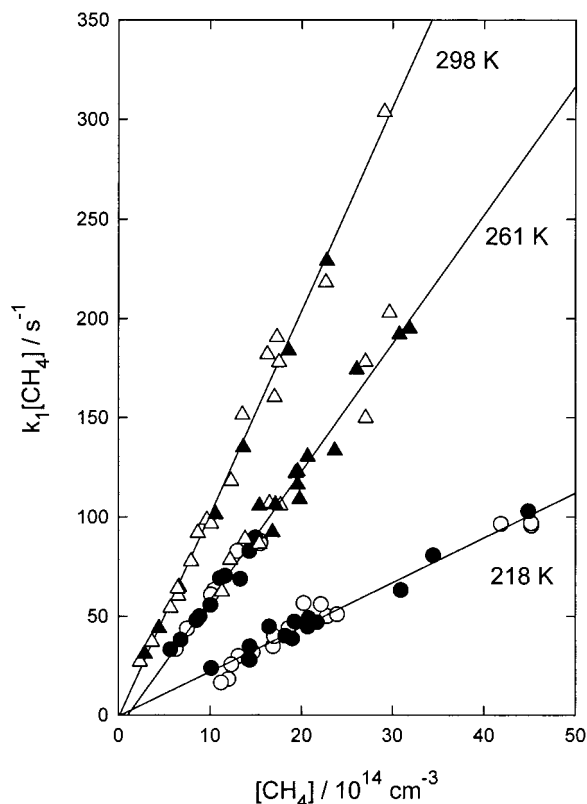


Figure 2. Plot of pseudo-first-order rate constant vs methane concentration; all of the data have been corrected for viscous pressure drop and diffusion (see text); open symbols are without added CF₄; filled symbols are with added CF₄; circles indicate experiments in which CH₄ was purified in situ (see text for details); triangles represent experiments in which CH₄ was not purified in situ; lines are least-squares fits of the data; temperatures are given next to each plot.

was observed, the initial slopes were used. Values of k_L were determined from the slopes of $\ln[I_0(\text{Cl})]$ vs l plots by linear least-squares analysis when no CH₄ was present in the system. Generally k_L was less than about 10% of k_+ . $I_0(\text{Cl})$ is the Cl atom fluorescence intensity without CH₄; it was measured by replacing the CH₄ flow with an equivalent flow of helium through the movable injector. A few minutes delay time was used after the CH₄ shut off in order to allow the flow system to stabilize. Then from eq 7, the pseudo-first-order rate constant, k_1' , is given by

$$k_1' = k_1[\text{CH}_4] = k_+ - k_L \quad (8)$$

A summary of observed rate constants is listed in Table 1 and shown in Figure 2.

No significant differences were observed between values obtained from the averages of individual $k_1'/[\text{CH}_4]$ points and from the slopes of k_1' vs $[\text{CH}_4]$ plots by linear least-squares

fitting. The Arrhenius plot shown in Figure 3 results in the following expression:

$$k_1 = (6.5 \pm 0.9) \times 10^{-12} \exp[(-1235 \pm 34)/T] \text{ cm}^3 \text{ molecule}^{-1} \text{ s}^{-1} \quad (9)$$

for $218 \leq T \leq 298$ K; the errors given are one standard deviation obtained from an unweighted least-squares analysis. Overall experimental uncertainty is estimated to be $\pm 15\%$.

Discussion

Spin Equilibration. Chlorine atoms can be in either the ground ²P_{3/2} or the excited ²P_{1/2} spin state, which is higher in energy by 882 cm⁻¹ (2.52 kcal/mole).^{33,34} In the stratosphere the spin states are expected to be in thermal equilibrium;³³ however, in the laboratory they may not be, and in order to apply measured rate coefficients to the atmosphere, it is important to check for spin equilibration. If Cl(²P_{1/2}) reacts with CH₄ at a rate sufficiently greater than Cl(²P_{3/2}), the spin distribution could affect the measurements. If interconversion



between the Cl states is rapid compared to reaction with CH₄, then spin equilibration can be maintained and the observed rate constant is at its maximum and is given by³⁴

$$k_1(\text{spin equilibrium}) = (k_{1a} + K \times k_{1b}) / (1 + K) \quad (10)$$

where the equilibrium constant, $K = 0.5 \exp(-2520/RT)$.

In the case of very slow interconversion, the two states decay independently with distinct rate constants, k_{1a} and k_{1b} . Even if the states are near equilibrium at the start of the Cl + CH₄ reaction (which might be the case in the present experiments because of a 50 ms delay between Cl formation and CH₄ addition), only a small fraction, 0.7% at 298 K, of Cl would be in the ²P_{1/2} state and the observed signal will be due mostly to the ²P_{3/2} state. Under slow spin equilibration conditions, the upper state would not be repopulated fast enough and the observed rate constant would be just k_{1a} , not the equilibrium rate constant (eq 10) needed for atmospheric models.

In a flash photolysis resonance fluorescence study of the Cl + CH₄ reaction, Ravishankara and Wine²¹ reported that at low temperatures the observed Cl losses depended on the composition of the reaction mixture. Under conditions where spin equilibration could be maintained—at low $[\text{CH}_4]$ (low Cl loss rates) or when efficient spin quenchers were present—they observed higher values for k_1' . They suggested that the differences among the various experimental techniques at low temperatures could be explained by the absence of quenchers and, thus, a non-Boltzmann distribution of the spin states in both the discharge flow and competitive chlorination studies.

Since measurements using the discharge flow technique are carried out at low pressures where diffusion is rapid, reactive species can undergo many wall collisions during their lifetime. Collision efficiencies less than 5×10^{-6} have been reported for deactivation of Cl(²P_{1/2}) on Teflon coated walls.³⁵ No spin deactivation rates have been reported for the wax coated walls used here; however, if they are as low as the reported values on Teflon, wall collisions would be too inefficient to equilibrate the states in our system. On the other hand, recent measurements of gas-phase spin quenching rates have shown that He and CH₄ itself are efficient quenchers of the ²P_{1/2} state.³³ To apply the

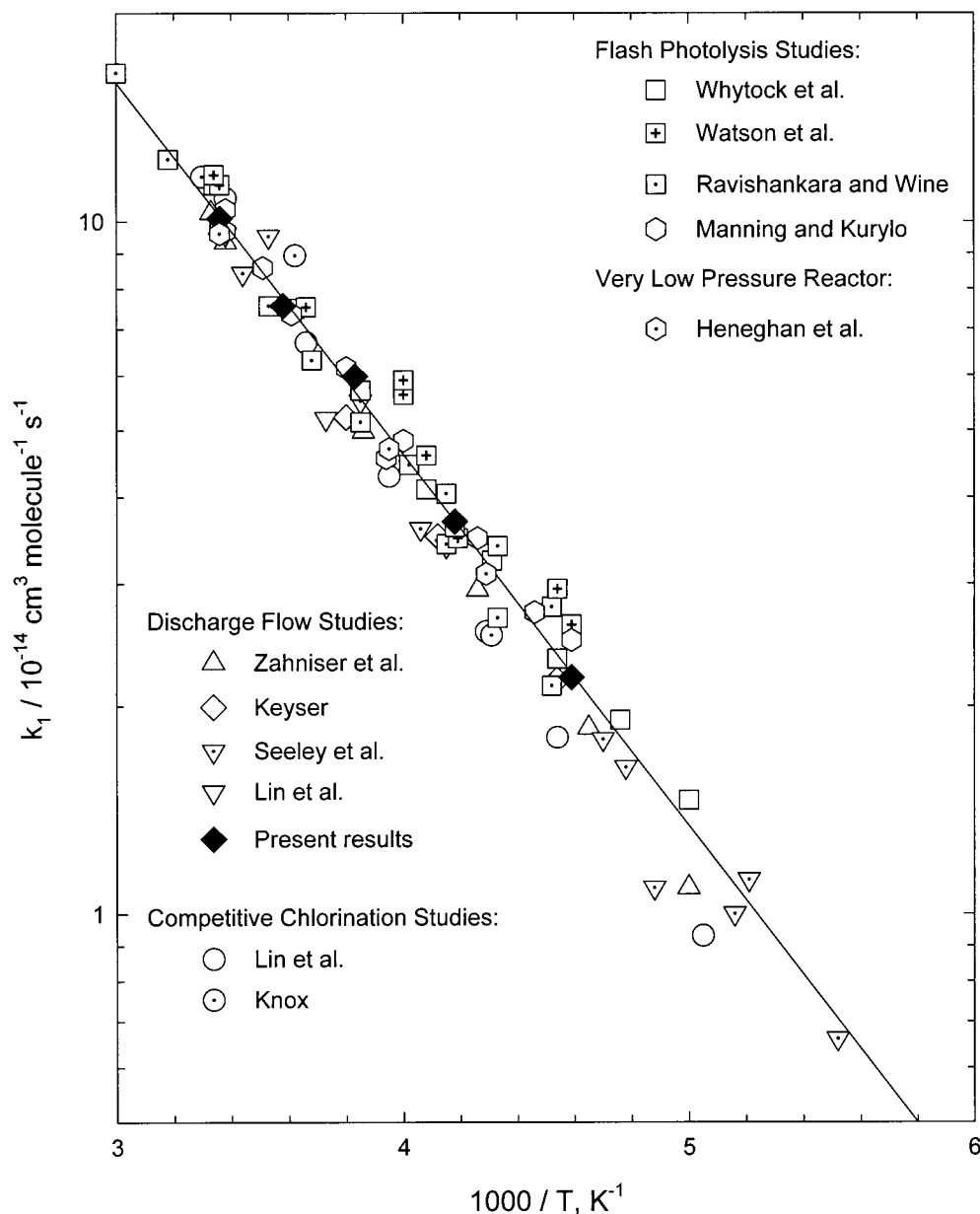
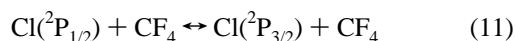


Figure 3. Arrhenius plot of present results compared to earlier studies using several experimental techniques. Absolute values for the competitive chlorination studies were calculated using $7.7 \times 10^{-11} \exp(-90/T) \text{ cm}^3 \text{ molecule}^{-1} \text{ s}^{-1}$ for the rate constant of the reference reaction, $\text{Cl} + \text{C}_2\text{H}_6$.¹² The line is the unweighted linear least-squares fit of the present results only.

discharge flow measurements of k_1 to stratospheric chemistry with confidence, it is crucial to confirm that Cl is indeed at thermal equilibrium under the conditions of the present study. Nonequilibrium could be revealed by nonlinear Cl decay curves and by changes in the observed rate constant when spin quenchers are added. At all temperatures studied, no significant curvature was observed in the $\ln[\text{Cl}]$ vs time plots. In addition, an efficient spin quencher, CF_4 , was added to the reaction



mixture to quench any excess $\text{Cl}(^2\text{P}_{1/2})$ and maintain spin equilibration. Measurements of the forward rate constant for reaction 11 average about $9 \times 10^{-11} \text{ cm}^3 \text{ molecule}^{-1} \text{ s}^{-1}$.^{33,36} CF_4 was added at concentrations averaging about $5.5 \times 10^{13} \text{ molecules cm}^{-3}$ to yield a quenching rate of nearly 5000 s^{-1} . Since there is about a 50 ms delay between the addition of CF_4 to Cl atoms and the start of the $\text{Cl} + \text{CH}_4$ reaction, there is more than sufficient time to bring the spin states into equilibra-

TABLE 2: Effect of Added Spin Quencher, CF_4 , on the Rate Constant, k_1

T (K)	k_1 ($10^{-14} \text{ cm}^3 \text{ molecule}^{-1} \text{ s}^{-1}$)			
	runs	without CF_4^a	runs	with CF_4^a
298	18	10.2 ± 0.68	6	10.0 ± 0.43
279	7	7.30 ± 0.80	5	7.92 ± 0.34
261	17	6.04 ± 0.45	21	5.94 ± 0.42
239	9	3.65 ± 0.17	4	3.77 ± 0.25
218	15	2.16 ± 0.33	14	2.25 ± 0.21

^a Errors are one standard deviation; average of individual $k_1'/[\text{CH}_4]$.

tion. Estimates and numerical simulations using the above quenching rate also show that most of the spin equilibration can be maintained by CF_4 alone even if k_{1b} is as much as 100 times greater than k_{1a} . In our system CH_4 and He also act to maintain the equilibrium.³³ The results of adding CF_4 are summarized in Table 2. No significant change in the rate constant was observed when quencher was added at temperatures from 218 to 298 K. These observations and simulations

show that the spin states were in thermal equilibrium in the present measurements.

Vibrational Deactivation. Recent theoretical and experimental studies have shown that the rate of reaction 1 is very sensitive to vibrational excitation of CH₄. Ab initio calculations using variational transition state theory predict that population of the umbrella bending mode (ν_4) near 1306 cm⁻¹ can increase the reaction rate over the ground state.³⁷ Enhancement factors as large as 16 and 52 are calculated at 300 and 200 K, respectively.²⁴ A molecular beam study at low collision energies has shown that speed distributions and spatial anisotropies of product CH₃ are consistent with reaction of CH₄ with vibrational excitation in the ν_4 mode and/or in the torsional mode (ν_2) near 1534 cm⁻¹; moreover, excitation to one of these modes enhances the reaction rate by a factor of 200.²⁵ At 298 K the thermal population of the two modes is 0.66%; at 218 K it is 0.062%. Because of the large enhancement, it is important that at the start of the reaction, the CH₄ vibrational population be the same as the nominal temperature of the carrier gas. In our system, CH₄ is precooled in the movable injector before it is added to Cl atoms. Residence times in the injector were 10 to 13 ms with average [CH₄] and [He] near 1.6×10^{16} and 3.7×10^{16} molecules cm⁻³, respectively. Vibrational deactivation can occur by wall collisions as well as by gas-phase collisions with He and CH₄ itself. Numerical simulations using quenching rate constants at 215 K of 1.1×10^{-14} and 6.2×10^{-15} cm³ molecule⁻¹ s⁻¹ for CH₄ and He collision partners,^{38,39} show that the 10–13 ms time period is sufficient to deactivate the 298 K population of the ν_2 and ν_4 modes and vibrational excitation should not interfere with our results.

Methyl Radical Reactions. To check for secondary chemistry involving methyl radicals, initial chlorine atom and methane concentrations were varied over a wide range. Since [Cl]₀ ≪ [CH₄], [Cl]₀ determines the maximum [CH₃] that can be produced and, hence, the importance of reactions 2 and 3. We can estimate the expected interference from reaction 2 at various concentrations by requiring the Cl atom loss by this reaction to be less than 10% of the loss by reaction 1. That is,

$$k_2[\text{CH}_3] < 0.1 k_1' \quad (12)$$

Since [CH₃] ≈ [Cl]₀, we have

$$[\text{Cl}]_0 \leq 0.1 k_1'/k_2 \quad (13)$$

Values for k_2 have been obtained at temperatures from 298 to 423 K by flash photolyzing mixtures of Cl₂, CH₄, and CO₂ and using UV absorption to monitor CH₃; computer simulations of [CH₃] vs time profiles and product analyses were then used to determine k_2 .⁴⁰ At 298 K k_2 was found to be 2×10^{-10} cm³ molecule⁻¹ s⁻¹ and is independent of CO₂ pressures between 50 and 300 Torr. For the purposes of the present discussion, we extrapolate these results to lower temperatures by using the reported temperature dependence; k_2 then is given by $3.7 \times 10^{-10} \exp(-185/T)$ cm³ molecule⁻¹ s⁻¹. Using this value for k_2 at 298 K, eq 13 becomes

$$[\text{Cl}]_0 \leq 5 \times 10^8 \times k_1' \quad (14)$$

To avoid interference, [Cl]₀ ≤ 1.2×10^{10} cm⁻³ for $k_1' = 25$ s⁻¹ and [Cl]₀ ≤ 1.5×10^{11} cm⁻³ for $k_1' = 300$ s⁻¹. Over the concentration ranges used in the present experiments, eq 14 predicts that some interference from reaction 2 is to be expected. This is confirmed by the plots in Figure 4, which show the

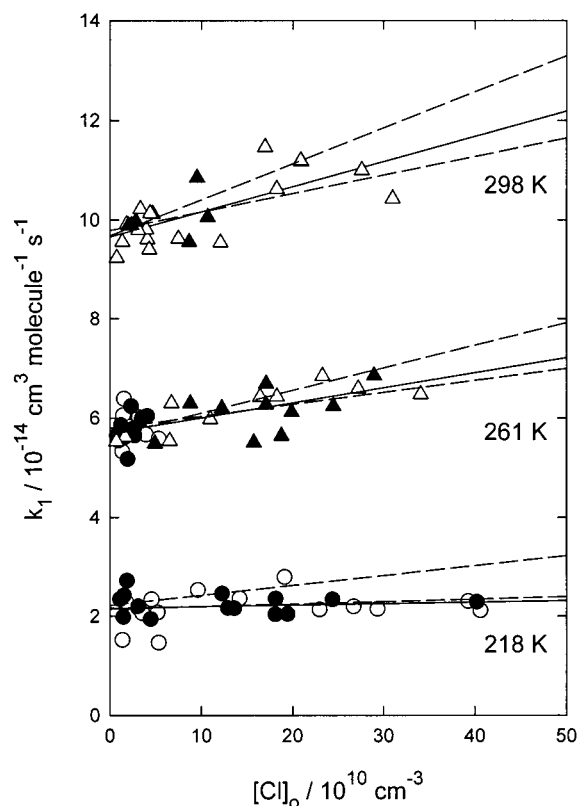


Figure 4. Plot of observed k_1 vs initial chlorine atom concentration; solid lines are linear least-squares fits to the data; dashed lines are obtained from numerical simulations described in the text; symbols have the same meaning as in Figure 2.

TABLE 3: Effect of Two Methods Used to Remove Interference from Reaction 2

T (K)	k_1 (10^{-14} cm ³ molecule ⁻¹ s ⁻¹) ^a		
	observed ^b	extrapolate to zero [Cl] ₀ ^c	exclude points simulations predict errors > 5% ^{b,d}
298	10.1 ± 0.60	9.66 ± 0.26	9.80 ± 0.14
261	5.98 ± 0.43	5.70 ± 0.08	5.81 ± 0.32
218	2.20 ± 0.28	2.16 ± 0.08	2.20 ± 0.30

^a Errors are one standard deviation. ^b Average of individual $k_1'/[\text{CH}_4]$. ^c See Figure 4. ^d See Figure 6.

change in observed k_1 as [Cl]₀ is increased at three temperatures; not enough data points were taken at 239 and 279 K to give reliable plots. At 298 K average values of k_1 , represented by the linear least-squares fit, increase by about 20% when [Cl]₀ varies from 1×10^{10} to 4×10^{11} cm⁻³; at 261 K the change is also about 20%, while at 218 K observed k_1 changes by only 6% over the same range of [Cl]₀. Since reaction 2 represents an added loss of Cl, the increase in observed k_1 with increasing [Cl]₀ indicates that this reaction may be interfering at high [Cl]₀. By extrapolating the k_1 vs [Cl]₀ curves to zero [Cl]₀, we can estimate k_1 free of interference from reaction 2. These values are compared to average values in Table 3. The extrapolated values are lower than the averages, but the effect is less than 5% at the three temperatures plotted. Computer simulations were used to further investigate interference from this reaction, and the results are discussed below.

Similar estimates can be made for reaction 3; in this case we have

$$k_3[\text{CH}_3][\text{Cl}_2] \leq 0.1 k_1[\text{Cl}][\text{CH}_4] \quad (15)$$

TABLE 4: Effect of Chlorine Atom Source and Purification of Methane

T (K)	k_1^a				k_1^a , purify CH ₄ in situ	
	microwave discharge		thermal		yes (17 runs)	no (21 runs)
	runs	source	runs	source		
279	6	7.94 ± 0.41	6	7.17 ± 0.75	5.79 ± 0.31	6.14 ± 0.45
261						
239	7	3.71 ± 0.12	6	3.66 ± 0.27		

^a 10⁻¹⁴ cm³ molecule⁻¹ s⁻¹; average of individual $k_1'/[\text{CH}_4]$; errors are one standard deviation.

noting that $[\text{CH}_3] \approx [\text{Cl}]$ and that $[\text{Cl}_2] = (1/2f_d)(1 - f_d)[\text{Cl}]_0$, we have

$$[\text{Cl}]_0 \leq (0.1/k_3)\{2f_d/(1 - f_d)\}k_1' \quad (16)$$

where f_d is the fractional dissociation of Cl₂, which ranges typically from about 0.25 to 0.55; for this estimate we take $f_d = 0.33$; using the literature value⁴¹ for k_3 : $5.0 \times 10^{-12} \exp(-267/T)$ cm³ molecule⁻¹ s⁻¹, at 298 K we have

$$[\text{Cl}]_0 \leq 5 \times 10^{10} k_1' \quad (17)$$

The minimum k_1' at 298 K was 27 s⁻¹ and this requires $[\text{Cl}]_0 \leq 1.3 \times 10^{12}$ cm⁻³ to prevent interference from reaction 3. The maximum $[\text{Cl}]_0$ used was 3.1×10^{11} cm⁻³, which is well below the estimate at 298 K. Similar results are found at the lower temperatures and these indicate that reaction 3 should not interfere with the present measurements.

Chlorine Atom Source. A microwave discharge was used to produce atomic Cl in most of the experimental runs. To minimize production of impurities, such as H or O atoms, most of the He flow bypassed the discharge region. If produced in sufficient concentrations, H atoms could interfere by forming atomic Cl by reaction 4. To check this possibility, a cleaner, thermal source of Cl atoms was used in some of the experiments. The results are summarized in Table 4. At both temperatures studied, no significant differences were observed using these two sources of atomic Cl. This shows that reaction 4 does not interfere with the present measurements.

Purification of Methane. Since C₂H₆ and higher alkanes react much more rapidly with Cl atoms than CH₄, it is important to use very high purity CH₄, especially at low temperatures. For example, at 298 K, k_5/k_1 is about 600 and at 218 K the ratio is about 2800. Thus, to keep interference from reaction 5 less than 1% requires that impurity levels of C₂H₆ in CH₄ be less than 17 and 4 ppm at 298 and 218 K, respectively. Batch analyses of the CH₄ supplied by the manufacturer found less than 1 ppm C₂H₆ and less than 2 ppm C₃H₈; these levels should prevent interference even at the lowest temperatures studied. However, to remove possible impurities added from the vacuum lines, CH₄ was purified in situ just upstream of its addition point during all (except for some runs at 261 K, see below) of the experiments below 298 K. This was done by passing the CH₄ through a molecular sieve (Linde 3A) trap at 195 K; earlier work showed that this method reduced C₂H₆ to less than 1 ppm with no trace of higher alkanes.^{14,15} At 261 K, in situ purification was done during 17 runs and no purification was done during 21 runs. The results are compared in the last two columns of Table 4; the difference is about 6% and does not appear to be significant even at the level of one standard deviation.

Computer Simulations. Numerical models were used to evaluate further the sensitivity of the Cl + CH₄ reaction system to secondary chemistry over a range of temperatures and reactant

TABLE 5: Reactions Used in Numerical Simulations

reaction	rate constant ^a	refs
Cl + CH ₄ → HCl + CH ₃	measured in this study, see text	
CH ₃ + Cl → CH ₃ Cl	$3.7 \times 10^{-10} \exp(-185/T)$	40
CH ₃ + Cl ₂ → CH ₃ Cl + Cl	$5.0 \times 10^{-12} \exp(-267/T)$	41
CH ₃ + CH ₃ + He → C ₂ H ₆ + He	$2.3 \times 10^{-30} T \exp(+185/T)$ at 1 Torr	45, 46
Cl + Cl + He → Cl ₂ + He	$6.1 \times 10^{-34} \exp(+906/T)$	27
Cl + wall → products	measured in this study, see text	
Cl + CH ₃ Cl → HCl + CH ₂ Cl	$3.2 \times 10^{-11} \exp(-1250/T)$	12
Cl + C ₂ H ₆ → HCl + C ₂ H ₅	$7.7 \times 10^{-11} \exp(-90/T)$	12
C ₂ H ₅ + Cl ₂ → Cl + C ₂ H ₅ Cl	$1.3 \times 10^{-11} \exp(+152/T)$	41
Cl + C ₂ H ₅ → HCl + C ₂ H ₄	2.4×10^{-10}	47
C ₂ H ₅ + C ₂ H ₅ → products	2.0×10^{-11}	48
CH ₃ + C ₂ H ₅ → products	5.0×10^{-11}	48
CH ₃ + wall → products	varies, see text	

^a Units are cm⁶ molecule⁻² s⁻¹ and cm³ molecule⁻¹ s⁻¹ for third-order and second-order reactions, respectively.

concentrations. The results can then be used to assess under which conditions the observed rate coefficients are free from significant interference. Most of the simulations were carried out using the Chemical Kinetics Simulator (CKS).⁴² In contrast to the customary numerical integration approach, CKS is based on a stochastic algorithm. The output from CKS was compared with results obtained by using two differential equation integrators based on standard Gear algorithms: ACUCHEM⁴³ and CHEMRXN.⁴⁴ The results from all three programs were essentially the same.

The reactions and rate constants listed in Table 5 were used to model the present study of Cl + CH₄ at 218, 261, and 298 K. Initial [Cl] and [CH₄] ranged over those used in the experimental runs. Input rate constants for reaction 1, $k_1(\text{in})$, were the values obtained by extrapolating to zero $[\text{Cl}]_0$ (see Figure 4 and Table 3). For Cl wall loss rates, we used the observed values given in the Experimental Section. The model output consists of [Cl] vs reaction time profiles. These were treated in the same way as experimental data to obtain the model prediction of k_1 : plots of ln [Cl] vs reaction time were fit by linear regression over time ranges similar to those used in the experiments; the slope gives a value for $-d \ln [\text{Cl}]/dt$ and, hence, from eq 7 a value for $k_1'(\text{out})$, and, knowing [CH₄], $k_1(\text{out})$ can be obtained.

As a first test of the model, we simulated the observed increase in k_1 with increasing $[\text{Cl}]_0$ by varying k_2 ; to make the system as sensitive as possible to CH₃ reactions we assumed that CH₃ wall loss is zero. As shown in Figure 5, the value of k_2 in the model must be greater than about 5×10^{-11} cm³ molecule⁻¹ s⁻¹ to fit the observations at 298 K. The best fit occurs in the range (1 to 2) × 10⁻¹⁰. This is close to the value of 2×10^{-10} cm³ molecule⁻¹ s⁻¹ reported by Timonen et al.⁴⁰ at 298 K, and, as a worst-case test for interference from reaction 2, we adopt this value along with their reported temperature dependence (see above and Table 5) in the rest of this discussion.

Except at very low [CH₄], the value of $k_1(\text{out})$ depends less strongly on [CH₄] than on $[\text{Cl}]_0$. Using this observation we can simplify the tests for interference from reaction 2 by setting [CH₄] at some intermediate value and fitting the model to the k_1 vs $[\text{Cl}]_0$ plots shown in Figure 4. The upper dashed lines near the plots for each temperature show the model results when CH₃ wall loss is set to zero; in this case the model results are more sensitive to $[\text{Cl}]_0$ than observed. The lower dashed lines are obtained by using 75, 50 and 150 s⁻¹ for the CH₃ wall loss at 298, 261 and 218 K, respectively. The best fit occurs at CH₃

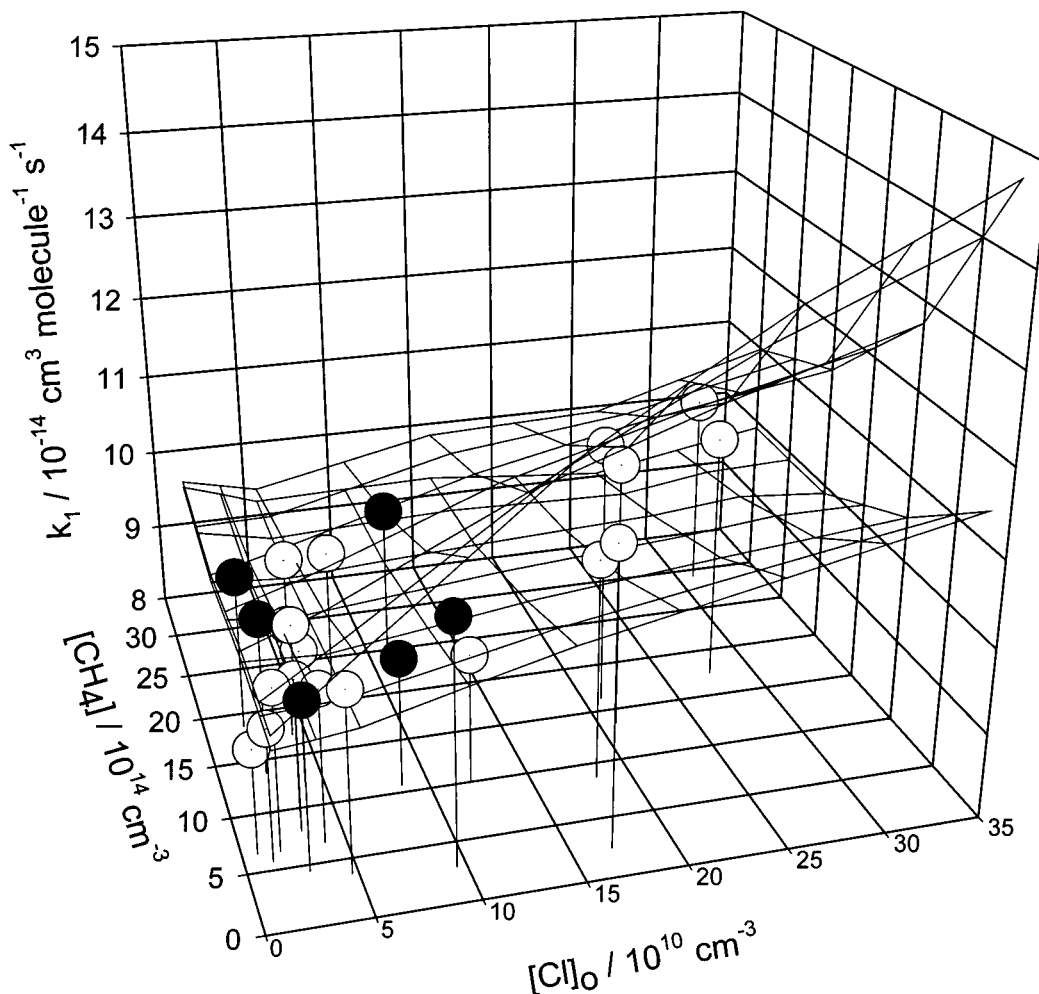


Figure 5. Plot of k_1 vs initial chlorine atom and methane concentrations at 298 K; filled and open symbols represent experiments with and without added CF_4 , respectively; lower and upper mesh plots are obtained from numerical simulations described in the text with k_2 set at 5×10^{-11} and $2 \times 10^{-10} \text{ cm}^3 \text{ molecule}^{-1} \text{ s}^{-1}$, respectively.

wall loss rate constants of 50, 40, and 150 s^{-1} ; these values correspond to wall loss collision efficiencies (γ) of 0.005, 0.004, and 0.1 at the three respective temperatures. What we call CH_3 wall loss could conceivably also include CH_3 reactions with impurities in the reaction mixture.

The models can now be used to estimate the degree of interference from secondary chemistry over various ranges of $[\text{Cl}]_0$ and $[\text{CH}_4]$ at each of the temperatures studied. In Figure 6 the best-fit model predictions for the percent changes in k_1 induced by secondary chemistry are plotted vs $[\text{Cl}]_0$ and $[\text{CH}_4]$. The percent change in k_1 is calculated using the relation, $\text{del}\% = \{[k_1(\text{out})/k_1(\text{in})] - 1\} \times 100\%$, where $k_1(\text{out})$ and $k_1(\text{in})$ are the input and output of the model discussed above. The results show that in order to avoid interference at the 10% level, $[\text{Cl}]_0$ should be less than about $1 \times 10^{11} \text{ atoms cm}^{-3}$ at 298 and 261 K and less than about $2 \times 10^{11} \text{ atoms cm}^{-3}$ at 218 K. Since the majority of the data points lie within the 5% contours at each of the three temperatures, the measured k_1 values should not be seriously affected. This can be tested by removing all data points beyond the 5% contours and recalculating the averages for k_1 . The results, shown in Table 3, are lower than the averages of all the data by less than about 3% and indicate that the present measurements should not be influenced significantly by secondary reactions.

Comparison with Theory and Earlier Experimental Results. The preexponential factor in the Arrhenius expression (eq 9) is in reasonably good agreement with the approximate value,

$8.3 \times 10^{-12} \text{ cm}^3 \text{ molecule}^{-1} \text{ s}^{-1}$, calculated from the thermochemistry of a collinear C–H–Cl transition state.¹⁸ A linear transition state is also predicted by ab initio calculations.^{49–51} Cold rotational state distributions observed in the product HCl also indicate a linear transition state.⁵²

The present results are in excellent agreement with earlier results from this laboratory¹⁵ using the same experimental technique but different flow tubes, flow meters, pressure gauges and temperature probes. In the earlier work the surface-to-volume ratio of the flow reactor was 1.6 cm^{-1} compared to the present value of 0.8 cm^{-1} ; also, the previous study used a phosphoric acid wall coating, not the halocarbon wax of the present study. The good agreement shows that wall effects such as a second-order surface reaction of Cl and CH_4 and calibration errors did not affect these measurements. The present measurements are also in very good agreement with the combined results of previous studies using discharge flow resonance fluorescence,^{14–16} discharge flow mass spectrometry,¹⁷ and very-low-pressure reactor¹⁸ techniques. At 298 and 220 K the present results are within 4 and 9%, respectively, of the combined data. These differences are within the expected experimental errors.

The average value of k_1 obtained near 220 K by the flash photolysis studies,^{19–22} after corrections for the small temperature differences and for 70 ppm C_2H_6 impurity in ref 20, is only about 6% higher than the present result. Estimates of vibrational quenching using the rate constants of Siddles et al.³⁸ show that, for bath gas pressures greater than 20 Torr, the

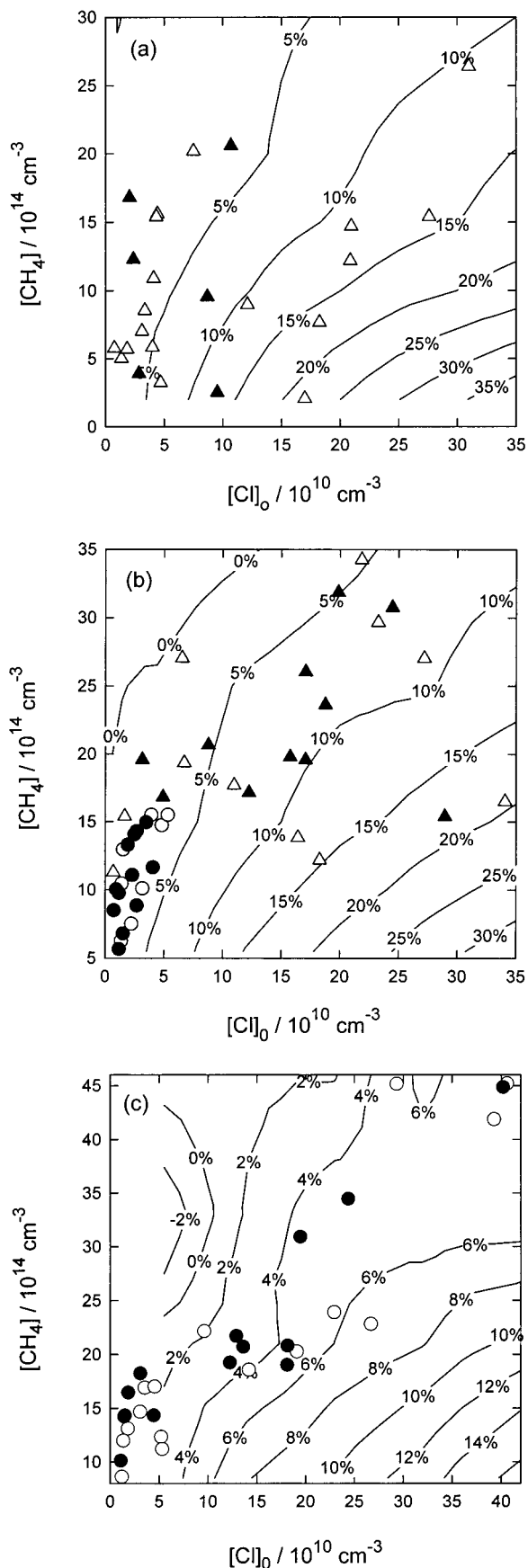


Figure 6. Increase in observed k_1 due to secondary chemistry as predicted by numerical simulations; contours are percent changes calculated from the relation: $\text{del}\% = (k_{\text{out}}/k_{\text{in}} - 1) \times 100\%$, where k_{in} and k_{out} are the input and output of the model; symbols are experimental data and have the same meaning as in Figure 2. Panel (a), 298 K; panel (b), 261 K; panel (c), 218 K.

lifetime of vibrationally excited CH_4 is less than about 1 ms. Manning and Kurylo²² used 5 Torr of argon as a bath gas, which gives vibrational lifetimes around 8 ms. These estimates represent upper limits to the lifetimes since CH_4 itself is an efficient vibrational quencher;³⁸ the good agreement among all of the flash photolysis results suggests that sufficient CH_4 was used to preclude interference from vibrationally excited CH_4 . Numerical simulations of the ground-state chemistry in the flash photolysis studies were done by using the CKS algorithm and the reactions in Table 5 but with rate constants and initial concentrations set at those used in the actual experiments. The results show no apparent interference from secondary chemistry, and the remaining differences may be due to combined experimental errors.

The competitive chlorination experiments¹⁷ should not be subject to interference from vibrationally excited CH_4 because of the high pressures used (high quenching rates), the length of time the reactants are held at low temperature with no addition of room-temperature CH_4 , and the low level of photolysis radiation injected. Numerical simulations of these experiments were carried out by using the CHEMRXN simulator. The reactions in Table 5 were used with the addition of a Cl_2 photolysis step, the reaction of Cl with C_2H_5Cl , and the back reactions of HCl with CH_3 and C_2H_5 radicals; the wall reactions were not included. Rate constants and conditions were set similar to the actual experiments. The model output values for the rate constant ratio, $R \equiv k(Cl + CH_4)/k(Cl + C_2H_6)$, differed from the input ratios by less than 1% at 296 and 220 K. This indicates that there was no interference from the ground-state chemistry included in the model. At 220 K our results are about 25% higher than the competitive chlorination results. If the errors in the ratio, R , are combined with errors in the reference rate constant, $k(Cl + C_2H_6)$, the competitive chlorination results overlap the present determination at the one sigma level. The reason for the 25% difference remains unclear; but, as the present study shows, it cannot be due to lack of spin or vibrational equilibration nor to known secondary chemistry.

Summary

The present study clearly demonstrates that the discharge flow measurements of the $Cl + CH_4$ reaction are not subject to systematic errors arising from nonequilibration of Cl atom spin states, vibrational excitation of CH_4 , or secondary chemistry. Addition of CF_4 at concentrations sufficient to bring about and maintain spin equilibrium resulted in no observable change in the $Cl + CH_4$ rate constant. CH_4 was vibrationally deactivated by precooling it before adding it to Cl atoms; the extent of the deactivation was checked by using numerical simulations with known vibrational quenching rate constants. Secondary chemistry due to impurities in the Cl atoms was checked by using both a microwave and a thermal source; impurities in the CH_4 source were minimized by using an in situ purification method. No significant difference was found in the results using either Cl atom source or purification of CH_4 . The secondary chemistry of CH_3 radicals produced in the $Cl + CH_4$ reaction was carefully examined by variation of the reactant concentrations in combination with numerical models. At the concentrations used in the present study, the results show that $Cl + CH_3$ interference is less than 3%; and in order to prevent interference at the 10% level, $[Cl]_0$ should be less than about 1×10^{11} atoms cm^{-3} .

Acknowledgment. The research described in this article was performed at the Jet Propulsion Laboratory, California Institute of Technology, under a contract with the National Aeronautics

and Space Administration. We thank W. B. DeMore for helpful discussions on this work.

References and Notes

- (1) Brasseur, G.; Solomon, S. *Aeronomy of the Middle Atmosphere*; Reidel: Dordrecht, 1984; Chapter 5.
- (2) Mickley, L. J.; Abbatt, J. P. D.; Frederick, J. E.; Russell, J. M., III *J. Geophys. Res.* **1997**, *102*, 21479.
- (3) Rinsland, C. P.; Gunson, M. R.; Salawitch, R. J.; Michelsen, H. A.; Zander, R.; Newchurch, M. J.; Abbas, M. M.; Abrams, M. C.; Manney, G. L.; Chang, A. Y.; Irion, F. W.; Goldman, A.; Mahieu, E. *Geophys. Res. Lett.* **1996**, *23*, 2365.
- (4) Douglass, A. R.; Schoeberl, M. R.; Stolarski, R. S.; Waters, J. W.; Russell, J. M., III; Roche, A. E.; Massie, S. T. *J. Geophys. Res.* **1995**, *100*, 13967.
- (5) WMO *Scientific Assessment of Ozone Depletion: 1994*; World Meteorological Organization Global Ozone Research and Monitoring Project, Report No. 37, Chapter 3.
- (6) Prather, M.; Jaffe, A. H. *J. Geophys. Res.* **1990**, *95*, 3473.
- (7) McElroy, M. B.; Salawitch, R. J.; Wofsy, S. C. *Planet. Space Sci.* **1988**, *36*, 73.
- (8) Salawitch, R. J.; Wofsy, S. C.; McElroy, M. B. *Geophys. Res. Lett.* **1988**, *15*, 871.
- (9) Bergamaschi, P.; Brühl, C.; Brenninkmeijer, C. A. M.; Saueressig, G.; Crowley, J. N.; Grooss, J. U.; Fischer, H.; Crutzen, P. J. *Geophys. Res. Lett.* **1996**, *23*, 2227.
- (10) Saueressig, G.; Bergamaschi, P.; Crowley, J. N.; Fischer, H.; Harris, G. W. *Geophys. Res. Lett.* **1996**, *23*, 3619. Saueressig, G.; Bergamaschi, P.; Crowley, J. N.; Fischer, H.; Harris, G. W. *Geophys. Res. Lett.* **1995**, *22*, 1225.
- (11) Müller, R.; Brenninkmeijer, C. A. M.; Crutzen, P. J. *Geophys. Res. Lett.* **1996**, *23*, 2129.
- (12) DeMore, W. B.; Golden, D. M.; Hampson, R. F.; Howard, C. J.; Kolb, C. E.; Kurylo, M. J.; Molina, M. J.; Ravishankara, A. R.; Sander, S. P. *Chemical Kinetics and Photochemical Data for Use in Stratospheric Modeling, Evaluation No. 12*; Jet Propulsion Laboratory, California Institute of Technology: Pasadena, CA, 1997; JPL Publication 97-4.
- (13) Atkinson, R.; Baulch, D. L.; Cox, R. A.; Hampson, R. F., Jr.; Kerr, J. A.; Rossi, M. J.; Troe, J., *J. Phys. Chem. Ref. Data* **1997**, *26*, 521 and earlier references cited therein.
- (14) Zahniser, M. S.; Berquist, B. M.; Kaufman, F. *Int. J. Chem. Kinet.* **1978**, *10*, 15.
- (15) Keyser, L. F. *J. Chem. Phys.* **1978**, *69*, 214.
- (16) Seeley, J. V.; Jayne, J. T.; Molina, M. J. *J. Phys. Chem.* **1996**, *100*, 4019.
- (17) Lin, C. L.; Leu, M. T.; DeMore, W. B. *J. Phys. Chem.* **1978**, *82*, 1772.
- (18) Heneghan, S. P.; Knoot, P. A.; Benson, S. W. *Int. J. Chem. Kinet.* **1981**, *13*, 677.
- (19) Whytock, D. A.; Lee, J. H.; Michael, J. V.; Payne, W. A.; Stief, L. *J. Chem. Phys.* **1977**, *66*, 2690.
- (20) Watson, R.; Machado, G.; Fischer, S.; Davis, D. D. *J. Chem. Phys.* **1976**, *65*, 2126.
- (21) Ravishankara, A. R.; Wine, P. H. *J. Chem. Phys.* **1980**, *72*, 25.
- (22) Manning, R. G.; Kurylo, M. J. *J. Phys. Chem.* **1977**, *81*, 291.
- (23) Knox, J. H. *Chem. Industry* **1955**, Dec. 10, 1631.
- (24) Duncan, W. T.; Truong, T. N. *J. Chem. Phys.* **1995**, *103*, 9642.
- (25) Kandel, S. A.; Zare, R. N. *J. Chem. Phys.* **1998**, *109*, 9719.
- (26) Appelman, E. H.; Clyne, M. A. A. *J. Chem. Soc., Faraday Trans.* **1975**, *1* (71), 2072.
- (27) Baulch, D. L.; Duxbury, J.; Grant, S. J.; Montague, D. C. *J. Phys. Chem. Ref. Data* **1981**, *10*.
- (28) Seeley, J. V.; Jayne, J. T.; Molina, M. J. *Int. J. Chem. Kinet.* **1993**, *25*, 571.
- (29) Kaufman, F. *Prog. React. Kinet.* **1961**, *1*, 1.
- (30) Keyser, L. F. *J. Phys. Chem.* **1984**, *88*, 4750.
- (31) Brown, R. L. *J. Res. Natl. Bur. Stand. (U.S.)* **1978**, *83*, 1.
- (32) Perry, R. H.; Chilton, C. H., Eds.; *Chemical Engineer's Handbook*, 5th ed.; McGraw-Hill: New York, 1973; p 3-230 f.
- (33) Tyndall, G. S.; Orlando, J. J.; Kegley-Owen, C. S. *J. Chem. Soc., Faraday Trans.* **1995**, *91*, 3055.
- (34) Clark, R. H.; Husain, D. *J. Chem. Soc., Faraday Trans. 2* **1984**, *80*, 97.
- (35) Müller-Markgraf, W.; Rossi, M. J. *J. Phys. Chem.* **1991**, *95*, 825.
- (36) Clark, R. H.; Husain, D. *J. Photochem.* **1983**, *21*, 93.
- (37) Espinosa-Garcia, J.; Corchado, J. C. *J. Chem. Phys.* **1996**, *105*, 3517.
- (38) Siddles, R. M.; Wilson, G. J.; Simpson, C. J. S. M. *Chem. Phys.* **1994**, *188*, 99.
- (39) Perrin, M. Y.; Jolicard, G. *Chem. Phys. Lett.* **1986**, *127*, 118.
- (40) Timonen, R.; Kalliorinne, K.; Koskikallio, J. *Acta Chem. Scand.* **1986**, *A 40*, 459.
- (41) Timonen, R. S.; Gutman, D. *J. Phys. Chem.* **1986**, *90*, 2987.
- (42) IBM, *CKS Chemical Kinetics Simulator*, IBM Almaden Research Center; IBM Corporation 1995 (Internet address is <http://eagle.almaden.ibm.com/st/>).
- (43) Braun, W.; Herron, J. T.; Kahaner, D. K. *Int. J. Chem. Kinet.* **1988**, *20*, 51.
- (44) Keyser, L. F. CHEMRXN, unpublished work.
- (45) Slagle, I. R.; Gutman, D.; Davies, J. W.; Pilling, M. J. *J. Phys. Chem.* **1988**, *92*, 2455.
- (46) MacPherson, M. T.; Pilling, M. J.; Smith, M. J. C. *Chem. Phys. Lett.* **1983**, *94*, 430.
- (47) Kaiser, E. W.; Rimai, L.; Wallington, T. J. *J. Phys. Chem.* **1989**, *93*, 4094.
- (48) Mallard, W. G.; Westley, F.; Herron, J. T.; Hampson, R. F.; Frizzell, D. H. *NIST Chemical Kinetics Data Base* **1998**, Version 2Q98.
- (49) Nyman, G.; Yu, H.-G.; Walker, R. B. *J. Chem. Phys.* **1998**, *109*, 5896.
- (50) Dobbs, K. D.; Dixon, D. A. *J. Phys. Chem.* **1994**, *98*, 12584.
- (51) Truong, T. N.; Truhlar, D. G. *J. Chem. Phys.* **1989**, *90*, 7137.
- (52) Simpson, W. R.; Rakitzis, T. P.; Kandel, S. A.; Lev-On, T.; Zare, R. N. *J. Phys. Chem.* **1996**, *100*, 7938.